Med Oncol _####################_
DOI 10.1007/s12032-015-0678-8

ORIGINAL PAPER

Screening of multi-targeted natural compounds for receptor tyrosine kinases inhibitors and biological evaluation on cancer cell lines, in silico and in vitro

Pushpendra Singh[1] · **Felix Bast**[1]

Received: 4 August 2015 / Accepted: 8 August 2015

Abstract Receptors for growth factors encompass within the superfamily of receptor tyrosine kinases and are known to regulate numerous biological processes including cellular growth, proliferation, metabolism, survival, cell differentiation and apoptosis. These receptors have recently caught the attention of the researchers as an attractive target to combat cancer owing to the evidence suggesting their over-expression in cancer cells. Therefore, we studied receptor-based molecular docking of IR (PDB; 3ETA), IGF1R (PDB; 1K3A), EGFR (PDB; 1M17), VEGFIR (PDB; 3HNG), and VEGFIIR (PDB; 2OH4) against natural compounds. Further, in vitro investigation of the biological effect of lead molecules in an array of cancer cell lines was done. All selected natural compounds were docked with the X-ray crystal structure of selected protein by employing GLIDE (Grid-based Ligand Docking with Energetics) Maestro 9.6. InterBioScreen natural compounds docked with each selected protein molecules by using GLIDE high throughput virtual screening. On the basis of Gscore, we select 20 compounds along with 68 anticancer compounds for GLIDE extra precision molecular docking. It was discovered in this study that compound epigallocatechin gallate (EGCG) yielded magnificent Gscore with IGF1R (PDB; 1K3A) and VEGFIIR (PDB; 2OH4), and protein–ligand interactions are chart out. Effect of EGCG on biological activity such as mRNA expression of selected protein, cell proliferation, oxidative stress, and cell migration was reported after the 48 h treatments in cancer cell lines. The RT-PCR densitometric bands analysis showed that compound EGCG reduced the mRNA expression of IGF1R, VEGFIIR, and mTOR at 80 μM concentration. Moreover, EGCG significantly reduced cell proliferation and ROS generation after 48 h treatments. Our result also indicated a reduction in the potential for cell migration that might show in vivo anti-metastasis activity of EGCG.

Keywords Cancer · InterBioScreen library · Natural compounds · Maestro 9.6 · In silico · In vitro

Introduction

Development of cancer multidrug resistance is a decisive factor in the defeat of copious chemotherapy including in blood cancers and solid tumors, such as breast, prostate, lung, and lower gastrointestinal tract cancers. Tumor cells are of two types: drug-sensitive and drug-unresponsive cells; cancer chemotherapy kills drug-sensitive cells but leaves drug-unresponsive cell. After cancer chemotherapy, drug-unresponsive cell develops drug resistant [1]. Radiotherapy can demolish healthy cells as well as destroy cancer cells and cause treatment side effects. Many factors are responsible for the development of drug resistance: (1) one or more mutations in target proteins, (2) increase in the activity of drug efflux pumps (ATP-binding cassette superfamily), (3) decreased drug influx, and (4) transformed expression of apoptosis and anti-apoptotic proteins [2]. Chemosensitization, radiosensitization, and cancer interception are a prerequisite for the enhancement of drug activity against cancer. Natural compounds and its derivatives, analogs, increase the chemosensitization and radiosensitization of drug [3]. Natural products are a prime source of new anticancer drugs and new drug leads. The plant-based development of anticancer agents including plants (vincristine and irinotecan), marine organisms (cytarabine and aplidine) and

✉ Felix Bast
felix.bast@gmail.com; felix.bast@cup.ac.in

[1] Centre for Biosciences, School of Basic and Applied Sciences, Central University of Punjab, Bathinda 151001, Punjab, India

Journal : Large 12032 | Dispatch : 19-8-2015 | Pages : 18
Article No. : 678 | ☐ LE | ☐ TYPESET
MS Code : MEDO-D-15-02328 | ☑ CP | ☑ DISK

microorganisms (dactinomycin and doxorubicin) added a new concept for cancer drug discovery. Comprehensive studies have confirmed that the most plentiful constituent in green tea is EGCG, which controls processes related to tumor development, highlighted in different cell lines systems, animal models and clinical trial [4–6]. The anticancer activity of EGCG may be accredited to the combinatory effects on multiple targets that are determinant for cell proliferation and apoptosis. Receptor tyrosine kinase such as epidermal growth factor (EGFR), insulin receptor (IR), insulin-like growth factor 1 receptor (IGF1R), and vascular endothelial growth factor receptor (VEGF2) are well known to synchronize many biological processes including cellular growth and apoptosis [7]. These receptors have recently caught the consciousness of the researchers as a stunning target to combat cancer owing to the proper documentation suggesting their over-expression on cancer cells. Number of reports confirm that, Green tea diminish the cell proliferation and promoted to cancer cell for growth inhibition in diverse cancer cells including colorectal, hepatocellular carcinoma cells, SW480 colon cancer cells, SV40 virally transformed WI38 human fibroblasts (WI38VA), prostate cancer, and Ishikawa cells [8–13].

Receptor tyrosine kinases (RTKs) are one of the most activated cell surface receptors for copious polypeptide growth factors, cytokines, and hormones that play a remarkable role in blood cancers and solid tumors [14]. RTKs have been shown not just to be the key regulators of normal cellular processes but additionally to imitate a critical role in the growth and development of a variety of cancer. Overexpression or overactivity of tyrosine kinase receptor has been described in some tumors, including prostate, breast, lung, and ovarian cancers. Several informative results demonstrated that a natural compound endeavors its anticancer activity by targeting cell surface protein molecules; the underlying molecular mechanisms are slightly understood. Moreover, multi-target-implicated therapeutics involves discovering a single agent that can work on two or more targets at the same time recently comes in the picture. It is speculated that this approach is pharmacologically more remarkable because of the easy accessible to the prediction of ADME/T properties of individual compounds. In the present study, we discover multi-targeted natural compounds for receptor tyrosine kinases inhibitors and biological evaluation of cancer cell lines by employing in silico and in vitro approach.

Materials and methods

Selection of ligand and protein molecules

Schematic diagram of the workflow study design is demonstrated in Fig. 1. Ligand molecules were selected in our study: (a) IBS natural compound library (InterBioScreen Ltd) and (b) anticancer natural compounds having anticancer activity are reported in published literature, but mechanism of action is still awaited [15–20]. These 68 anticancer natural compounds (Table 1) are reported in our previously published article [21, 22]. Ligands were prepared by using LigPrep module of the Maestro 9.6 application. LigPrep performs many corrections on the ligands, such as the addition of hydrogens, 2D–3D conversion, corrected bond lengths and bond angles, low-energy structure, and ring conformation. Apart from that another parameter such as ionization does not change, tautomers not created and retain particular charities generate at most one per ligands were used as a default parameter in Maestro 9.6. After that all atom force field charges and atom types were assigned by the optimized potential for liquid simulations (OPLS_2005) force field [23–25]. Finally, one conformation for each ligand was generated, and ligands are ready for docking. The X-ray structure of the IR (PDB; 3ETA), IGF1R (PDB; 1K3A), EGFR (PDB; 1M17), VEGFIR (PDB; 3HNG), VEGFIIR (PDB; 2OH4), and AR (PDB; 2PIV) is retrieved from the protein data bank. Maestro 9.6 protein preparation wizard application was performed for the correction of raw PDB structure, where changes such as addition of hydrogen atoms, assigning bond orders, creation of zero-order bonds to metal, creation of disulfide bonds, fixing of the charges and orientation of groups were incorporated into the raw PDB structure.

Molecular docking

In silico molecular docking protocol was adapted from our published literature [21–24]. Receptor-based molecular docking was conducted using GLIDE software from Schrödinger suite [25–27]. Each of these compounds was docked into target protein accordingly with positions, orientations, and conformations of the ligand in the receptor binding site, and the docking structure possessing the lowest energy was preferred. We studied receptor-based molecular docking of IR (PDB; 3ETA), IGF1R (PDB; 1K3A), EGFR (PDB; 1M17), VEGFIR (PDB; 3HNG), and VEGFIIR (PDB; 2OH4) against natural compounds. In the present study, we screened approximately 50,000 natural compounds from the IBS. All natural compounds were docked with the X-ray crystal structure of chosen protein by employing GLIDE Maestro 9.6. IBS natural compounds docked with every selected protein molecules by using HTVS. In order to provide a better correlation between right poses and good scores, GLIDE-XP mode was subsequently used on the conformations selected from HTVS mode. On the basis of Gscore, we select 20 compounds along with 68 anticancer compounds for GLIDE-XP molecular docking. After the completion of ligands and

Journal : Large 12032 Dispatch : 19-8-2015 Pages : 18
Article No. : 678 LE TYPESET
MS Code : MEDO-D-15-02328 CP DISK

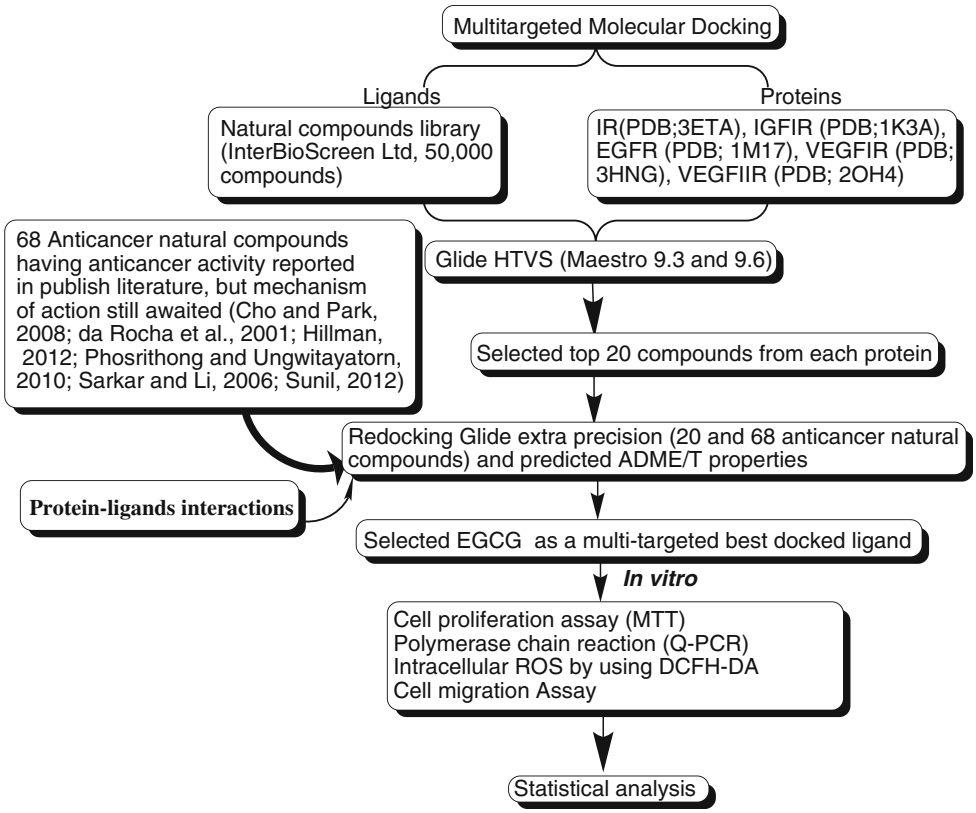

Fig. 1 Workflow of screening of multitargeted compound and biological effect in cancer cell lines

proteins preparation, a receptor grid file was generated. For running the grid generation module, we have scaled van der Waal radii of receptor atoms by 1.00 Å with a partial atomic charge of 0.25 as default setting of Maestro 9.6. The active site of the receptor maintain a precise scoring function with thermodynamically most favorable energy and is calculated on a grid by various sets of fields. After the formation of the receptor grid file, flexible ligands with rigid-receptor-based molecular docking were performed. The best-fit compounds have been chosen for each target by optimal energy value and types of interactions.

Absorption, distribution, metabolism, excretion, and toxicity (ADME/T) properties studies

The majority of drug candidates do not succeed in clinical trials due to poor toxicology assessments (ADME/T). Thus, ADME/T properties of best-docked compounds were predicted using QikProp application of Maestro 9.6 (structural, physicochemical, biochemical, pharmacokinetics, and toxicity properties). It predicts intrinsic properties of the molecules (drug-like properties) such as octanol/water partition, log BB, overall CNS activity, log IC50 for Herg K+ channel blockage, Caco-2, MDCK cell permeability and logKhsa for human serum albumin binding [28, 29].

Reagents

DMEM media, 1 % penicillin/streptomycin, and fetal bovine serum (FBS) were procured from Invitrogen, and Ham's F-12 media were from Himedia. EGCG was purchased from MP Biomedicals Pvt Ltd and dissolved in dimethylsulfoxide (DMSO) as a 20MM stock solution. The final dilution was done in culture medium at a DMSO concentration of 0.25 % (vol/vol).

Cell lines

Hepatocellular carcinoma (HepG2), lung carcinoma (A549 and H460) and prostate cancer (PC3), and human cell lines were procured from NCCS, Pune, India. Cells were grown in NCCS recommended phenol red media containing 10 % FBS and 1 % penicillin/streptomycin and have to maintain in a 37-centigrade incubator with 5 % CO_2 humidified atmosphere.

Total RNA isolation, cDNA synthesis, and quantitative RT-PCR

One million cells per well were plated in the six-well culture plate media supplemented with 10 % FBS and 1 % penicillin and streptomycin and then incubated at 37 °C

Journal : Large 12032 Dispatch : 19-8-2015 Pages : 18
Article No. : 678 LE TYPESET
MS Code : MEDO-D-15-02328 CP DISK

Table 1 List of PubChem molecules screened in this study with structural and physicochemical parameters (21, 22)

S.N.	Comp. (CID)	Mol. wt. (130–725)	Volume (500–2000)	H-bond donor (0–6)	H-bond accp. (2–20)	QPlogP oct (8.0–35.0)	QPlog Pw (4.0–45.0)	QPlog $P_{o/w}$ (−2.0 to 6.5)	QPlogS mol/L(−6.5 to 0.5)
1	73641	488.706	1431.329	4	7.1	25.992	14.438	4.231	−5.37
2	73659	472.707	1414.592	3	5.4	23.674	11.514	5.168	−6.242
3	91469	242.274	798.666	2	2.25	13.082	8.215	2.761	−3.579
4	245005	645.745	1754.494	3	16.95	33.013	22.138	1.963	−2.418
5	259846	426.724	1378.31	1	1.7	17.885	4.492	7.043	−7.907
6	261265	430.626	1387.41	2	6.15	21.018	10.026	4.381	−6.176
7	440917	136.236	621.544	0	0	5.044	−0.203	3.99	−4.003
8	441794	496.553	1351.712	5	12.35	28.735	20.523	1.144	−3.268
9	442793	294.39	1090.905	1	4.2	13.232	5.745	3.766	−4.42
10	445154	228.247	786.572	3	2.25	13.599	9.347	2.012	−2.803
11	176870	393.441	1226.24	1.5	7.4	18.347	10.736	3.942	−4.335
12	10184653	485.945	1449.822	2	9.45	25.015	14.39	3.847	−5.269
13	208908	581.06	1674.641	1	8.25	26.434	13.376	5.881	−6.837
14	5328779	294.309	980.124	3	5.5	17.809	12.771	1.849	−4.481
15	123631	446.908	1262.744	1	7.7	19.692	10.252	3.898	−3.559
16	932	272.257	840.858	2	4	14.728	10.219	1.658	−3.47
17	2044	305.173	871.406	1	3.75	12.522	6.462	2.434	−4.415
18	2543	310.435	1122.807	1	1.5	13.745	4.396	5.604	−6.637
19	3220	270.241	808.031	1	4.25	12.607	8.522	1.258	−3.07
20	5350	177.279	661.995	0	6.5	9.242	8.882	0.535	0.827
21	9064	290.272	872.256	5	5.45	19.89	15.596	0.481	−2.609
22	10494	456.707	1401.838	2	3.7	21.162	8.308	6.238	−7.067
23	16078	314.467	1147.852	1	1.5	13.759	3.962	5.694	−6.774
24	64945	456.707	1387.747	2	3.7	20.965	8.275	6.125	−6.917
25	65064	458.378	1255.716	8	8.75	31.171	23.925	−0.24	−3.547
26	68077	372.374	1098.572	0	6.25	15.512	7.736	3.31	−3.466
27	72276	290.272	872.747	5	5.45	19.683	15.562	0.494	−2.587
28	72277	306.271	892.592	6	6.2	21.772	17.64	−0.17	−2.356
29	72281	302.283	919.955	2	4.75	15.742	10.473	1.803	−3.782
30	72326	442.724	1393.324	2	3.4	20.187	7.483	5.92	−6.784
31	446925	536.882	2240.509	0	0	21.45	−4.618	19.06	−21.136
32	457964	338.486	1040.152	4	5.85	19.237	12.383	1.916	−3.138
33	3035241	323.822	1004.466	2.5	6.25	17.869	11.099	2.03	−2.845
34	5270604	426.724	1374.435	1	1.7	18.141	4.741	7.024	−8.012
35	5280343	302.24	883.724	4	5.25	18.67	14.544	0.522	−3.1
36	5280373	284.268	860.146	1	3.75	13.02	8.02	2.522	−3.523
37	5280443	270.241	822.143	2	3.75	14.898	10.217	1.644	−3.374
38	5280445	286.24	843.558	3	4.5	16.591	12.301	0.96	−3.096
39	5280789	538.898	2258.34	0	0	21.818	−4.468	19.12	−21.322
40	5280863	286.24	840.186	3	4.5	16.394	12.278	1.059	−3.057
41	5280896	264.321	879.908	2	4.75	13.913	8.701	2.18	−2.772
42	5280899	568.881	2125.203	2	3.4	25.936	5.687	10.56	−12.471
43	5280961	270.241	807.798	2	3.75	14.142	9.887	1.678	−3.014
44	5281605	270.241	818.653	2	3.75	15.089	10.185	1.757	−3.317
45	5281607	254.242	799.678	1	3	12.869	8.121	2.386	−3.647
46	5281612	300.267	901.458	2	4.5	15.652	10.473	1.79	−3.694
47	6441009	785.023	2136.644	9	21.15	48.098	33.717	1.359	−2.85
48	6857485	276.504	1033.576	0	0	10.507	−0.266	8.832	−9.421

Journal : Large 12032 Dispatch : 19-8-2015 Pages : 18
Article No. : 678 □ LE □ TYPESET
MS Code : MEDO-D-15-02328 ✔ CP ✔ DISK

Table 1 continued

S.N.	Comp. (CID)	Mol. wt. (130–725)	Volume (500–2000)	H-bond donor (0–6)	H-bond accp. (2–20)	QPlogP oct (8.0–35.0)	QPlog Pw (4.0–45.0)	QPlog $P_{o/w}$ (−2.0 to 6.5)	QPlogS mol/L(−6.5 to 0.5)
49	11353973	479.965	1419.846	2	6.4	24.197	12.538	5.001	−7.537
50	11476171	439.559	1456.758	2	3.25	22.132	9.911	6.748	−8.739
51	11640390	421.501	1336.398	3	4.75	24.019	13.923	5.015	−7.393
52	24785538	461.501	1398.675	3	7.5	26.47	15.152	4.164	−6.935
53	46881851	439.559	1458.756	2	3.25	22.144	9.957	6.742	−8.831
54	56603750	678.82	1960.352	8	14	41.827	28.302	2.644	−5.369
55	57390076	515.66	1691.49	4	8	29.212	15.987	4.552	−6.261
56	5281614	286.24	841.842	4	5.5	18.889	14.744	0.5	−2.796
57	5281616	270.241	817.4	2	3.75	14.551	10.181	1.794	−3.308
58	5281670	302.24	858.752	4	5.25	19.268	14.332	0.41	−2.755
59	5281672	318.239	882.348	5	6	20.432	16.443	−0.28	−2.564
60	6917781	805.013	2188.868	5	14.05	39.445	21.319	6.229	−6.364
61	9548699	274.489	963.039	0	0	9.861	−0.523	8.186	−8.689
62	9548711	278.52	1081.566	0	0	10.365	−1.273	9.272	−9.918
63	9825149	453.586	1502.475	2	5.25	23.868	11.935	5.735	−7.262
64	9910986	401.846	1141.405	2	6.7	20.745	12.793	2.369	−3.673
65	5281707	268.225	774.132	2	4.5	14.593	10.923	1.319	−2.915
67	5281708	254.242	787.865	2	4	14.141	10.264	1.774	−2.957
68	6436722	542.93	2281.771	0	0	22.431	−4.283	18.96	−21.565

Compounds: PubChem molecules screened in this study

Molecular weight (<500 Da)

Volume: estimated number of hydrogen bonds that would be accepted by the solute from water molecules in an aqueous solution. Values are averages taken over a number of configurations, so they can be non-integer

Hydrogen bond donors (<5)

Hydrogen bond acceptors (<10)

QP log Poct: predicted partition coefficient of octanol/gas (8.0–35.0)

QP log Pw: predicted partition coefficient of water/gas (4.0–45.0)

Plog Pw: predicted octanol/water partition co-efficient log p (recommended range −2.0 to 6.5)

QPlog S: predicted aqueous solubility; S in mol/L (acceptable range −6.5 to 0.5)

overnight with 5 % Co_2. Cells were exposed to EGCG 80 μM for 48 h. After 48 h, total RNA was extracted using TRI reagent (Life Technologies, Gaithersburg, MD, USA). RNA was quantified by 260/280 nm absorbance and agarose gel electrophoresis. Yield and purity were verified by absorbance (optical density), and the absorption ratio A260 nm/A280 nm between 1.93 and 2.06 was taken into consideration for cDNA preparation. For cDNA synthesis, 1 μg of total RNA was reverse-transcribed into cDNA using a high-capacity PrimeScript first-strand cDNA Synthesis Kit (Takara Bio Inc). cDNA, stored at −80 °C prior to PCR amplification, was amplified using the DNA amplification kit (Genei). List of primers used in this study for RT-PCR shown in Table 2. Consequently, gene expression was quantified by RT-PCR by using Veriti® 96-well fast thermal cycler (Applied Biosystems). The cycling parameters were optimized as follows: start at 60 °C for 2 min, followed by activation at 95 °C for 5 min, denaturing at 95 °C for 30 s, annealing at 60 °C for 45 s, and elongation at 72 °C for 45 s, repeated for 40 amplification cycles [30]. Products of RT-PCR obtained were separated by gel electrophoresis to confirm correct amplification and size. Water was used to detect primer–template cDNA interactions. Further, GAPDH and β-actin were used as a housekeeping gene to assure equal loading of the sample. Gel picture was taken by using automated image-capture and analyzed using system Gel Doc™ XR with Image Lab™ Software. Gel band intensities of PCR product were then calculated with Bio-Rad's Image Lab software tool.

Protocol for MTT assay

MTT assays were performed to evaluate the cell inhibitory effects of EGCG on A549 and PC3 cells. Approximately 7×10^3 cells per well were seeded in 96-well plates with

Journal : Large 12032 Dispatch : 19-8-2015 Pages : 18
Article No. : 678 ☐ LE ☐ TYPESET
MS Code : MEDO-D-15-02328 ☑ CP ☑ DISK

Table 2 Primer sets used for amplification

Sr. no.	Name of gene	Forward primer (5′–3′)	Reverse primer (5′–3′)
1	VEGFR-2	5′GCGGGCTCCTGACTACAC3′	5′CCAAATGCTCCACCAACTCTG3′
2	IGF1R	TTAAAATGGCCAGAACCTGAG	ATTATAACCAAGCCTCCCAC
3	mTOR	CCAACAGTTCACCCTCAGGT	GCTGCCACTCTCCAAGTTTC
4	EGFR	5′ATGCCCGCATTAGCTCTTAG3′	5′GCAACTTCCCAAAATGTGCC3′
5	Bcl-2	CATGTGTGTGGAGAGCGTCAA	GCCGGTTCAGGTACTCAGT CA
6	Bid	GCTGTATAGCTGCTTCCAGTGTA	GCTATCTTCCAGCCTGTCTTCTC
7	β-Actin	GTGGGGCGCCCCAGGCACCA	CTCCTTAAGTCACGCACGATTTC
8	GAPDH	ACGGATTTGGTCGTATTGGGCG	CTCCTGGAAGATGGTGATGG

media containing 10 % FBS and 1 % penicillin and streptomycin. After 24-h incubation, the media were discarded and added FBS free media for serum starvation. The cells were exposed to the EGCG containing 5 % media and incubated for 48 h. At the end of the incubation period, media were disposed of, and 100 µl of MTT (0.5 mg/ml) in PBS was added. Cells were incubated at 37 °C for 4 h. The supernatant was removed from the wells, and the reduced MTT dye was dissolved with 200 µl/well DMSO. Absorbance was measured by using fluorescence microplate reader (Synergy/H1) with a wavelength of 570 nm.

Determination of intracellular reactive oxygen species (ROS)

The levels of ROS were determined quantitatively by using 2, 7-dichlorodihydrofluorescein diacetate (DCFH-DA). 7×10^3 cells per well were plated in the 96-well tissue culture media containing 10 % FBS and 1 % penicillin/streptomycin and then incubated at 37 °C with 5 % CO_2 overnight. After 24-h incubation, the media were discarded and FBS free media were added to carry out serum starvation. Next day, the media were replaced with 200 µL of fresh complete medium containing varying concentrations of compounds. After 48 h, the supernatants were removed, and cell layers were washed with PBS and incubated after re-suspending in 100 µL 5 µM CM-H_2DCFDA, and the plates were placed into an incubator for 4 h. Subsequently, the fluorescence intensity was measured at an excitation wavelength of 485 nm and emission wavelength of 530 nm using a fluorescence microplate reader (Synergy/H1).

Cell migration assay (in vitro wound-healing assay)

In vitro, the wound-healing assay was performed as described previously [31, 32]. In brief, cells were seeded in a six-well plate and grown overnight to the confluence. After 24 h, cultures were replaced with fresh medium containing 0.5 % FBS (control) or the same medium containing concentration-dependent treatment EGCG. Monolayer cells were scratched with a-200 µL pipette tip to create a wound and kept in a 37 °C containing 95 % air and 5 % CO_2. After 48 h, cells were washed twice with DMEM to remove floating cells. The rate of wound closure was assessed and photographed after 48 h, and scale bars to images using ImageJ were added.

Statistical analysis

Statistical values are expressed as the mean ± SEM (SigmaPlot). The significance of the difference between the control and each experimental test condition was analyzed by Kruskal–Wallis one-way analysis of variance on ranks followed by Tukey's multiple range tests. The value of $p < 0.05$ was considered statistically significant.

Results and discussion

EGCG has excellent Gscore when docked with proteins IGF1R and VEGFIIR

This study is a concentrated to explore the potent multi-targeted inhibitor against RTKs employing molecular docking approach. Molecular docking of IR, IGF1R, EGFR, VEGFI, and VEGFII RTKs against natural compounds has been carried out. First, we performed HTVS of IBS against the IR, IGF1R, EGFR, VEGFIR, and VEGFIIR. Further, 20 best compounds from each protein molecules that possess minimal Gscore along with 68 natural compounds molecular docking were performed using the XP mode of GLIDE. In the present investigation, our result highlighted that EGCG yielded a preeminent dock score for proteins IGF1R and VEGFR-2. Protein–ligand interactions accentuated that the lipophilic, hydrogen bonding, π–π stacking, and cation–π interactions represent a ruling contribution at the active site. Molecular docking operation distinguishes the foremost docking free energy value (Gscore) against these receptor molecules. Deliberated Gscore from molecular docking yielded minimum energy for EGCG with proteins IGF1R and VEGFR2, −9.72 and −11.03 kcal/mol, respectively. Nevertheless,

Journal : Large 12032 Dispatch : 19-8-2015 Pages : 18
Article No. : 678 LE TYPESET
MS Code : MEDO-D-15-02328 CP DISK

Table 3 Lowest binding energy for the ligand–IGF1R (PDB, 1K3A) protein interaction as detected by GLIDE molecular docking

Ligand type	Compounds ID	Gscore	Lipophilic Evdw	H bond	Electro	Protein–ligand interactions
IGFR, tyrosine kinase inhibitors (control)	CID11353973	−5.83	−4.11	−1.96	−0.69	Gly 976, Gln977, Met1052, and Asp1123
	CID46881851	−5	−3.46	−1.66	−0.72	Lys1003 and Gln977
	CID9825149	−4.84	−3.52	−1.58	−0.68	–
	CID3035241	−4.82	−2.72	−1.42	−0.67	Lys1003
Anticancer natural compounds	CID65064	−9.72	−2.77	−5.33	−2	Gln977, Lys1003, Glu1050, Met1052, and Asp1123
	CID441794	−7.84	−3.34	−3.5	−1.09	Asp1056
	CID5281670	−7.82	−2.11	−4.18	−1.42	Leu975, Gln977, and Gly1122
	CID5281672	−7.68	−1.38	−4.35	−1.86	Leu975, Gly1122, and Asp1123
	CID6917781	−7.42	−3.25	−3.24	−1.07	Lys1003, Glu1013, Arg1012, and Asp1056
IBS	STOCK1N-54535	−10.73	−3.64	−5.54	−1.94	Glu1050, Met1052, Asp1056, and Asp1123
	STOCK1N-61631	−10.28	−3.91	−5.07	−2	Asp1056 and Asp1123
	STOCK1N-50260	−9.95	−3.66	−4.81	−2	Glu1050, Met1052, Asp1056, and Asp1123
	STOCK1N-57549	−9.71	−3.23	−4.59	−2	Asp1056 and Asp1123
	STOCK1N-68861	−9.42	−2.34	−3.4	−1.25	Glu1050 and Met1052

Table 4 Lowest binding energy for the ligand–VEGFR-2 (PDB, 2OH4) protein interaction as detected by GLIDE molecular docking

Ligand type	Compounds ID	Gscore	Lipophilic Evdw	H bond	Electro	Protein–ligand interactions
VEGFR2, inhibitors (control)	CID6450551	−11.45	−5.47	−1.38	−0.77	Lys866, Glu883, Val912, Glu915, and Phe1045
	CID11525740	−9.32	−6.05	−1.37	−0.59	Lys866 and Cys917
	CID3081361	−7.36	−5.1	−1	−0.18	Cys917 and Phe1045
	CID9809715	−4.05	−2.47	−1.6	−0.7	–
Anticancer natural compounds	CID5280343	−11.07	−4.69	−2.84	−1.24	Lys866, Glu883, Val912, Cys917, and Phe1045
	CID65064	−11.03	−5.02	−3.8	−1.08	Ala864,Glu883, Val912, Glu915, and Asp1044
	CID5280445	−10.83	−4.83	−2.37	−1.19	Lys866, Glu883, Val912, Cys917, and Phe1045
	CID5281672	−10.76	−3.69	−3.82	−1.48	Lys866, Glu883, Asp1044, and Phe1045
	CID72277	−10.75	−4.18	−3.77	−1.49	Lys866, Glu883, Val912, Cys917, and Phe1045
IIBS	STOCK1N-24948	−12.31	−6.5	−5	−2.97	Lys866, Glu883, Val912, Cys917, and Phe1045
	STOCK1N-08247	−11.9	−5.57	−4.51	−1.32	Glu883, Val912, Cys917, Asp1044, and Phe1045
	STOCK1N-75618	−11.79	−2.99	−5.44	−1.36	Glu883
	STOCK1N-69130	−11.63	−5.45	−5.75	−1.33	Cys917 and Asp1044
	STOCK1N-74472	−11.56	−4.78	−6.51	−1.24	Cys917, Asp1044, and Phe1045

Journal : Large 12032 Dispatch : 19-8-2015 Pages : 18
Article No. : 678 LE TYPESET
MS Code : MEDO-D-15-02328 CP DISK

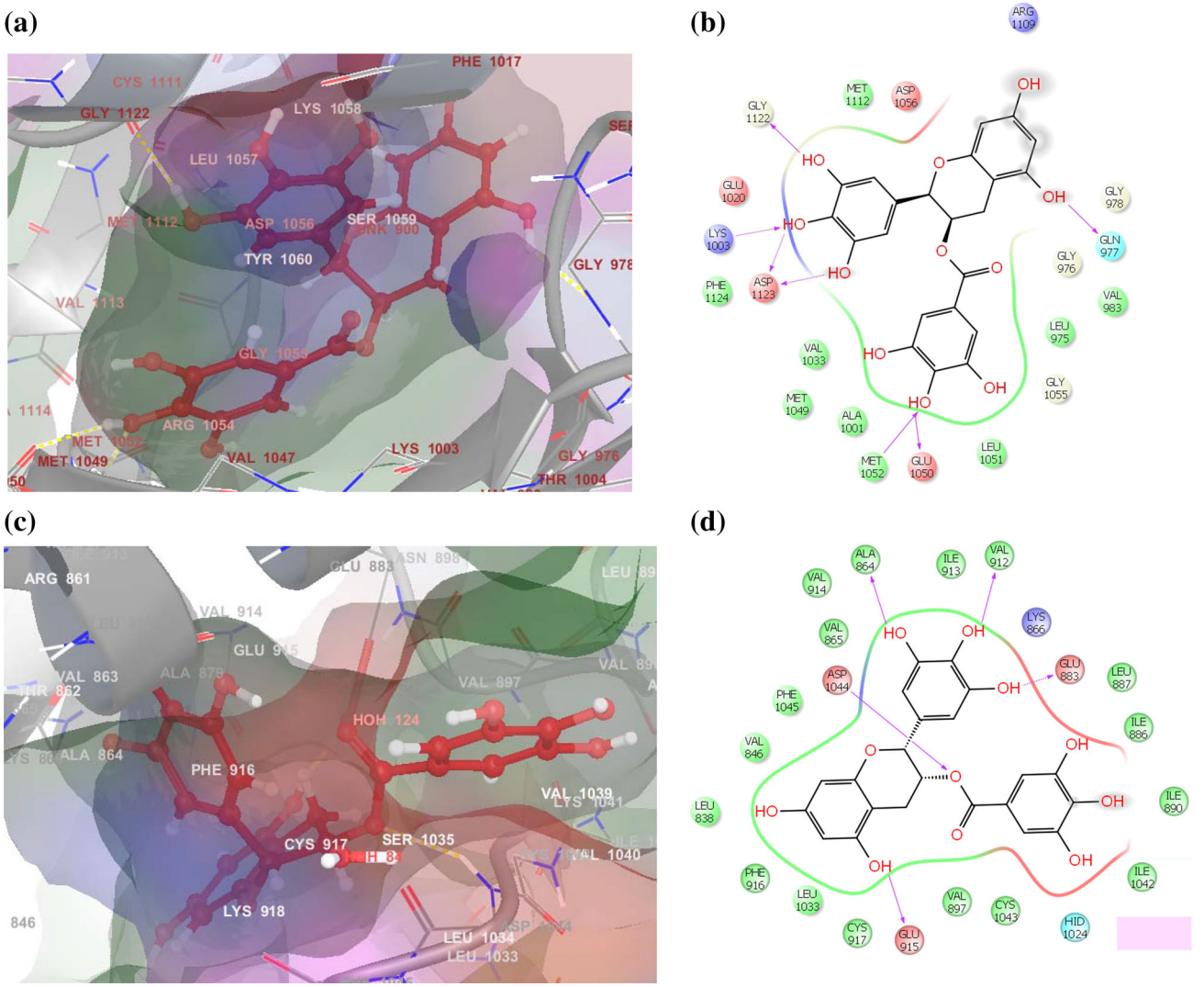

Fig. 2 **a** *Ribbon* presentation of IGF1R (PDB; 1K3A) protein molecule with CID65064, **b** protein–ligand interactions profile of 1K3A with CID65064, **c** *ribbon* presentation of VEGFR-2 (PDB; 20H4) protein molecule with CID65064, **d** protein–ligand interactions profile of 20H4 with CID65064

this study tremendously introduces novel classes of multi-target natural compounds. The crystal structure of the IGF1R (PDB, 1K3A) has been determined by 2.1-Å resolution. Furthermore, the structure of the 1K3A complex with EGCG highlighted that the lipophilic, electrostatic hydrogen bond, π–π stacking, and cation–π interactions are key contributors in protein–ligand interactions. Protein–ligand interactions of 1K3A with EGCG showed that amino acids Val983, Leu975, Ala1001, Val1033, Met1049, Leu1051, Met1052, Met1112, and Phe1124 appeared in the hydrophobic interactions. Furthermore, amino acids Lys1003 and Asp1123 were involved in side-chain hydrogen bond formation, whereas amino acids Gln977, Glu1050 and Met1052 in backbone hydrogen bonding of protein–ligand interactions (Table 3). Moreover, the crystal structure of the VEGFIIR (PDB, 2OH4) has been determined by 2.05 Å resolutions. Further, it was observed that amino acids Leu838, Val846, Ala864, Val865, Ile1086, Ile890, Phe916, Cys917, Ile913, Val914, Leu1033, Cys1043, and Phe1045 form hydrophobic interactions during protein–ligand interactions of 2OH4 with EGCG. Consequently, it was shown that amino acid Glu883 was included in side-chain hydrogen bonding and amino acids Ala864, Val912, Glu915, and Asp1044 involved in backbone hydrogen bonding (Table 4). Moreover, IBS natural compounds STOCK1N-54535, STOCK1N-61631, STOCK1N-50260, STOCK1N-57549, and STOCK1N-68861 have better Gscore −10.73, −10.28, −9.95, −9.71, and −9.42 kcal/mol, respectively, when docked with 1K3A. However, STOCK1N-24948, STOCK1N-08247, STOCK1N-75618, STOCK1N-69130, and STOCK1N-74472 have excellent Gscore −12.31,

Journal : Large 12032 Dispatch : 19-8-2015 Pages : 18
Article No. : 678 LE TYPESET
MS Code : MEDO-D-15-02328 CP DISK

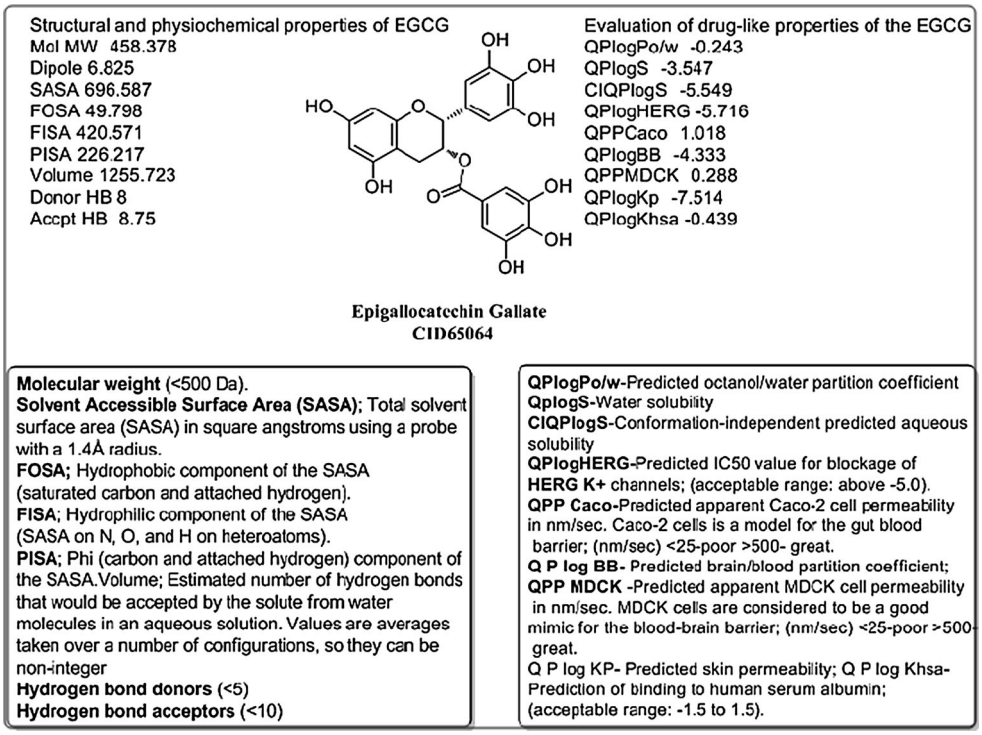

Fig. 3 ADME/T properties. Structural, physicochemical, biochemical, pharmacokinetics, and toxicity properties of compound EGCG were examined by using the QikProp application of Maestro 9.6

−11.9, −11.79, −11.63, and −11.56, respectively, when docked with 2OH4. Interestingly, none of these compounds have better Gscore for both protein IK3A and 2OH4 (Fig. 2).

ADME/T properties

Pharmacokinetic properties of multi-targeted natural compound EGCG were examined by using the QikProp application of Maestro 9.6 [36] and underlined in Fig. 3. Compound EGCG was found to be promising based on their docking free energy score and binding mode. The most fascinating aspect of EGCG is their admirable, Qplogpo/w, Qplogs, CIQPlogS, QplogHERG, QplogBB, Qplogkp, and Qplogkhsa value −0.243, −3.547, −5.549, −5.716, −4.333, −7.514, and −0.439, respectively, which satisfy the Lipinski's rule of five, whereas QPPCaco and QPPMDCK are not satisfactory 1.018 and 0.288, respectively; structure modification may be required to enhance these activities (Fig. 3). Moreover, polar surface area, high oral bioavailability, H-bond donors and acceptors are imperative criteria for the development of therapeutic agents. Veber et al. 2002 reported that compounds having 10 or fewer rotatable bonds and polar surface area equal to or less than 140 Å (or 12 or fewer H-bond donors and acceptors) may have a high probability for best oral bioavailability in the rat. Furthermore, it is also reported that polar surface area is inversely proportional to permeation rate [37]. Compound EGCG has 773.184 SASA values that are claimed to be suitable for therapeutic agents. These results indicate that this compound will have better penetration rate.

Effect of EGCG on IGF1R and VEGFIIR mRNA expression in cancer cell lines

We investigated whether EGCG could impede IGF1R and VEGFIIR expression in HepG2, H460, A549, and PC3 cells. Cells were incubated for 48 h with EGCG and determine the mRNA expression by using RT-PCR. The primer sets used for amplification are listed in Table 2. As shown in Fig. 4, RT-PCR demonstrates that EGCG has a potential for robust inhibition of IGF1R and VEGFIIR. The activity of IGF1R and VEGFIIR has been shown to play a critical role in cancer cell proliferation. The Q-PCR densitometric bands analysis showed that compound EGCG reduced the mRNA expression of IGF1R by 49 % in HepG2 ($^{***}P < 0.001$), 49 % in A549 ($^{*}P < 0.05$), 22 % in H460 ($^{*}P < 0.05$), and 61 % in PC3 cells at 80 μM concentration, whereas EGCG reduced the mRNA expression of VEGFR2 by 21 % in HepG2 ($^{**}P < 0.01$), 30 % in A549, 20 % in H460, and 25 % in PC3 ($^{**}P < 0.01$) cells at 80 μM concentration. Moreover, EGCG reduced the mRNA expression of mTOR by 40 % in GepG2 ($^{*}P < 0.05$), 30 % in A549, 32 % in H460 ($^{*}P < 0.05$), and 20 % in PC3 cells at 80 μM concentration. Furthermore, pro-apoptotic proteins Bid and anti-apoptosis protein (Bcl-2) mRNA expression was determined by RT-PCR. EGCG reduces the Bcl2 expression and induces the pro-apoptotic mRNA Bid expression.

Journal : Large 12032 Dispatch : 19-8-2015 Pages : 18
Article No. : 678 LE TYPESET
MS Code : MEDO-D-15-02328 CP DISK

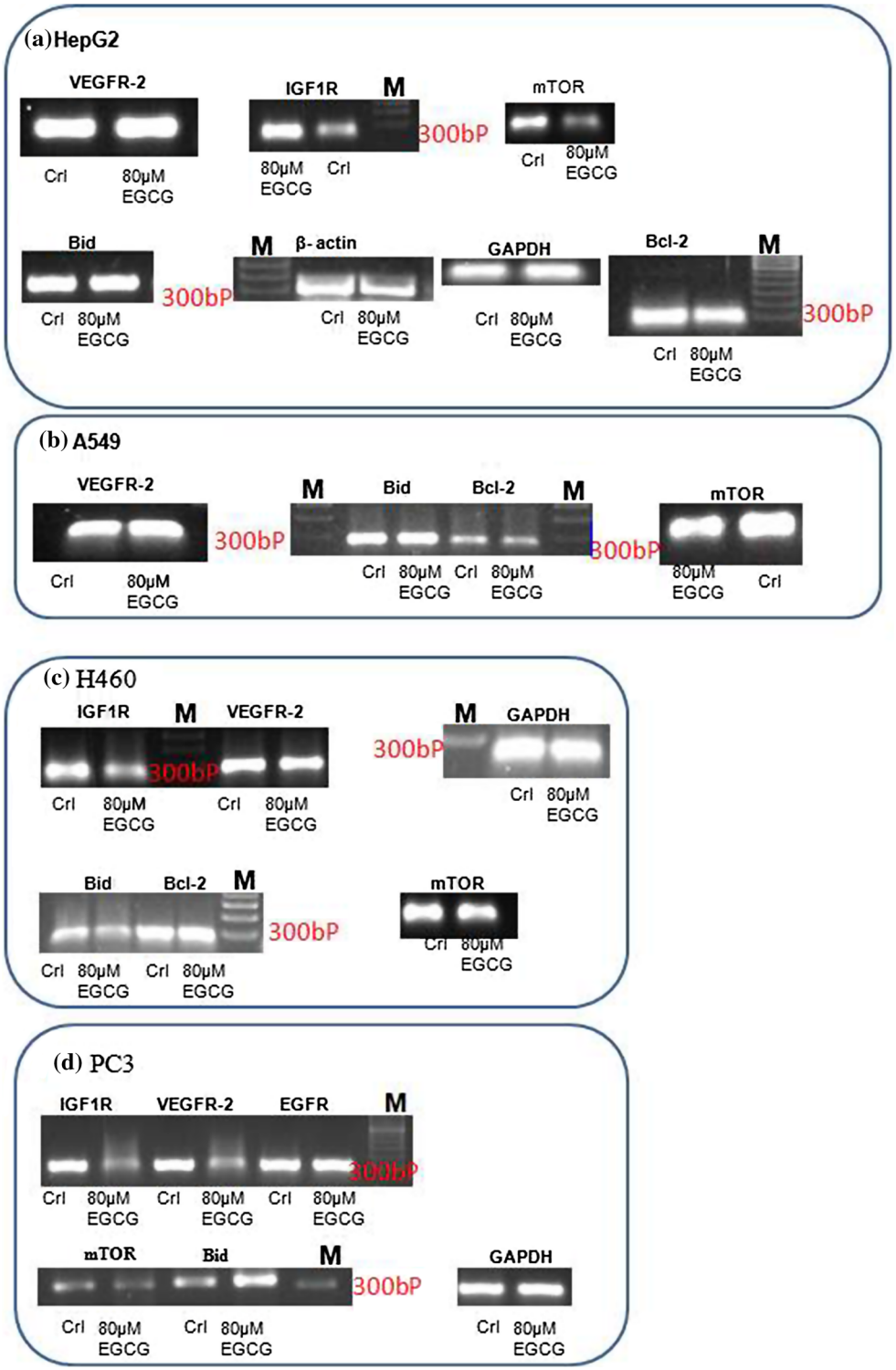

Fig. 4 Effect of EGCG on IGF1R, VEGFR-2, mTOR, Bid, and Bcl2 mRNA turnover in selected four cells. **a**, **b**, **c**, and **d** represented gel band in HepG2, A549, H460, and PC3, respectively. Cells were treated with 80 μM EGCG for the indicated time periods. IGF1R, VEGFR-2, mTOR, Bid, and Bcl2 mRNA levels were determined by RT-PCR and normalized to β-actin and GAPDH as the loading control. mRNA of IGF1R, VEGFR-2, mTOR, Bid, and Bcl2 has changed in cells treated with EGCG. EGCG down-regulated the expression of IGF1R, VEGFR-2, and mTOR (**e**, **f**, **g**). Moreover, EGCG up-regulated the expression of apoptotic mRNA product Bid but inhibited the expression of anti-apoptotic mRNA products Bcl-2 (**h**, **i**)

Journal : Large 12032 Dispatch : 19-8-2015 Pages : 18
Article No. : 678 ☐ LE ☐ TYPESET
MS Code : MEDO-D-15-02328 ☑ CP ☑ DISK

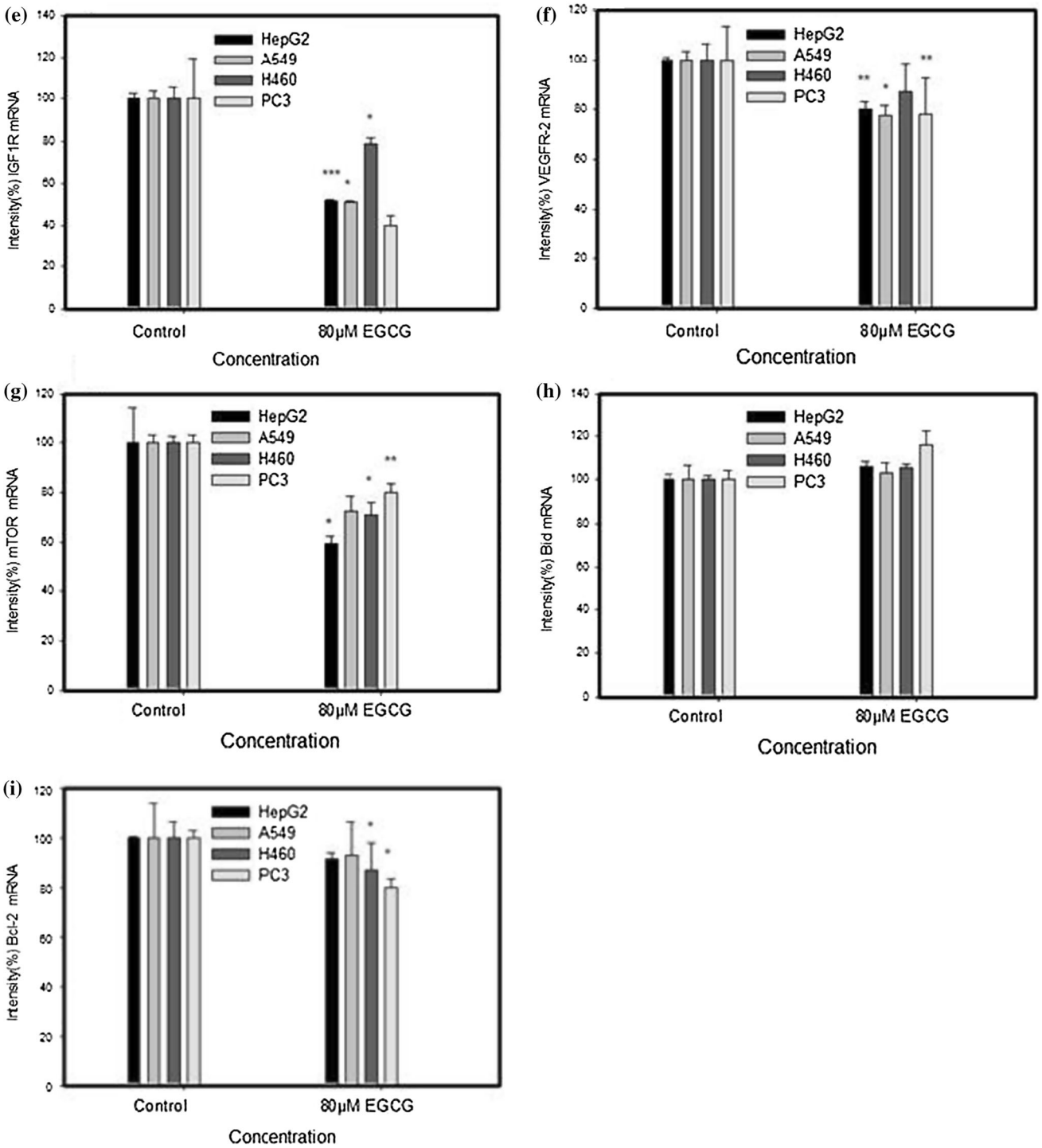

Fig. 4 continued

Interestingly, previously it is reported that EGCG treatment does not affect VEGF expression and angiogenesis in the normal tissues. Nevertheless, oral EGCG treatment inhibits angiogenesis and VEGF expression in the same mice [33]. Moreover, EGCG treatment increases hepatic autophagy by the emergence of autophagosomes and restorative autophagic flux in hepatic cells and in vivo [34].

Effects of EGCG on cell growth and ROS in cancer cell lines

To measure the cytotoxicity of EGCG in cancer cells, MTT assay was performed. A549 and PC3 cells were cultured with 5, 10, 20, 40, and 80 μM EGCG for 48 h. EGCG exhibited a remarkable reduction in cell proliferation in

Journal : Large 12032 Dispatch : 19-8-2015 Pages : 18
Article No. : 678 LE TYPESET
MS Code : MEDO-D-15-02328 CP DISK

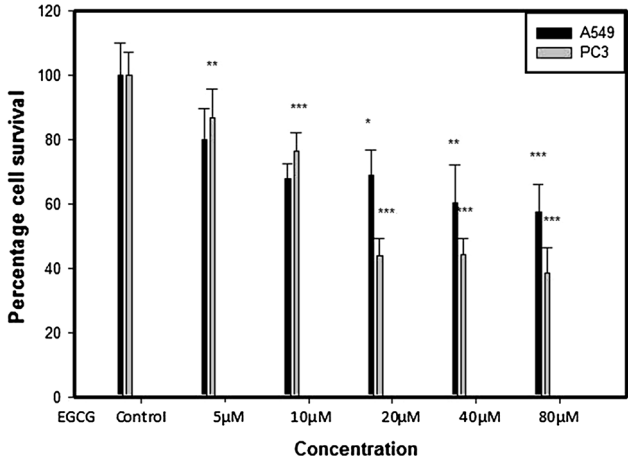

Fig. 5 A549 and PC3 cells were cultured with 5, 10, 20, 40, and 80 μM EGCG for 48 h. Effect of EGCG on the cell growth in A549 and PC3 cells. EGCG reduces the cell growth of the A549 and PC3 cells in a dose-dependent manner determined by the MTT assay

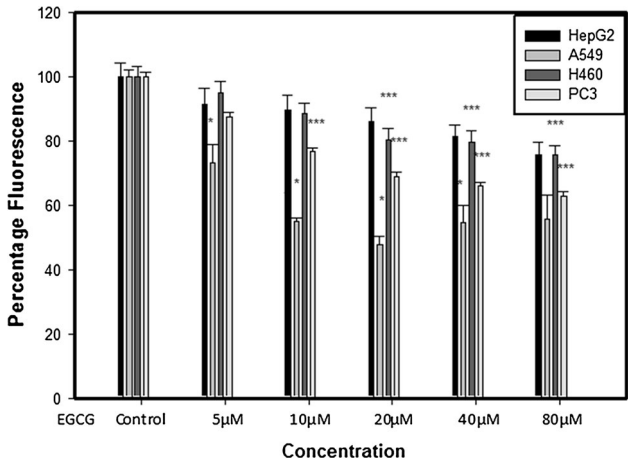

Fig. 6 EGCG reduces ROS level in the HepG2, A549, H460, and PC3 cells in a dose-dependent manner determined by the CM-H2DCFDA fluorescent-based assay. $*P < 0.05$, $**P < 0.01$, and $***P < 0.001$ versus controls

these cells in a concentration-dependent manner. Consistently, it was more pronounced at concentrations between 5 and 80 μM. The mean 50 % inhibitory concentration of EGCG on cell growth was at 40 μM in A549 cells for 48 h treatment, whereas in PC3 cells, EGCG significantly reduced 50 % cell viability at 20 μM concentration. Effect of EGCG on HepG2 and H460 cells also reduces cell proliferation reported in our article [24]. The conversion of nonfluorescent CM-H2DCFDA to fluorescent DCF was used for the detection of the intracellular production of ROS. EGCG exposure led to significant changes in relative ROS were observed on cancer cell lines after 48 h treatments. HepG2, A549, H460, and PC3 cells were cultured with 5, 10, 20, 40, and 80 μM EGCG for 48 h and calculated the ROS reduction. The mean 50 % ROS reduction at 20 μM on A549 cells, whereas in PC3 cells, 40 % ROS reduction at 40 μM concentration. EGCG induced apoptosis via generation of ROS, which guides to the activation of P-38 and caspase-3 on human endometrial adenocarcinoma cells [35] (Figs. 5, 6).

Effects of EGCG on cell migration of cancer cells (in vitro)

Flavonoid derivatives including EGCG, synthetic flavonoid WYC02-9, and apigenin-dependent cell migration assay delineated in different cancer cells [36]. Various reports indicated that, by employing an in vitro migration assay, treatment of 4T1 mammary carcinoma with EGCG resulted in concentration-dependent inhibition of cell migration [36]. Furthermore, the wound-healing assay showed that EGCG appreciably reduced the cell migration of melanoma cells in a dose-dependent manner from 20 to 100 μM. Thus, EGCG may be an encouraging compound for the prevention of metastasis of uveal melanoma [37]. Synthetic flavonoid WYC02-9 influences cell cytotoxicity on cervical cancer cells and has the apprehensive effect on cell migration in vitro and in vivo via MAPK14 pathway [38]. Representative photomicrographs of the HepG2 and PC-3 cells after the treatment with different concentrations of EGCG are shown in Fig. 7a, c and the cell migration assay in Fig. 7b, d, respectively. The rate of wound closure was photographed after 48 h and scale bars to images were added using ImageJ. The figure shows that width of wound increases effectively after the treatment of EGCG for 48 h.

Green tea is a glorious beverage with health benefits with abundant polyphenols including epigallocatechin gallate (EGCG), epicatechin gallate (ECG), epigallate catechin (EGC), and epicatechin. EGCG affects numerous molecular targets involved in cancer cell proliferation and survival. Previous studies have established that active anticancer constituent in green tea is EGCG with the anticancer activity highlighted in various in vitro and in vivo studies. The anticancer activity of EGCG may be accredited to the combinatory effects on multiple targets that are determinant for cell proliferation and apoptosis. Interestingly, green tea reduces the cell proliferation and sensitizes the cell for apoptosis and cell cycle arrest including colorectal and hepatocellular carcinoma cells, via regulating the activation of tyrosine kinase EGFR [39, 40]. Furthermore, it is reported that EGCG has potently inhibitory effects on tumor angiogenesis induced by IGF1 in non-small cell lung cancer cells via downregulation of HIF-1α and VEGF expression [41].

Journal : Large 12032 Dispatch : 19-8-2015 Pages : 18
Article No. : 678 LE TYPESET
MS Code : MEDO-D-15-02328 CP DISK

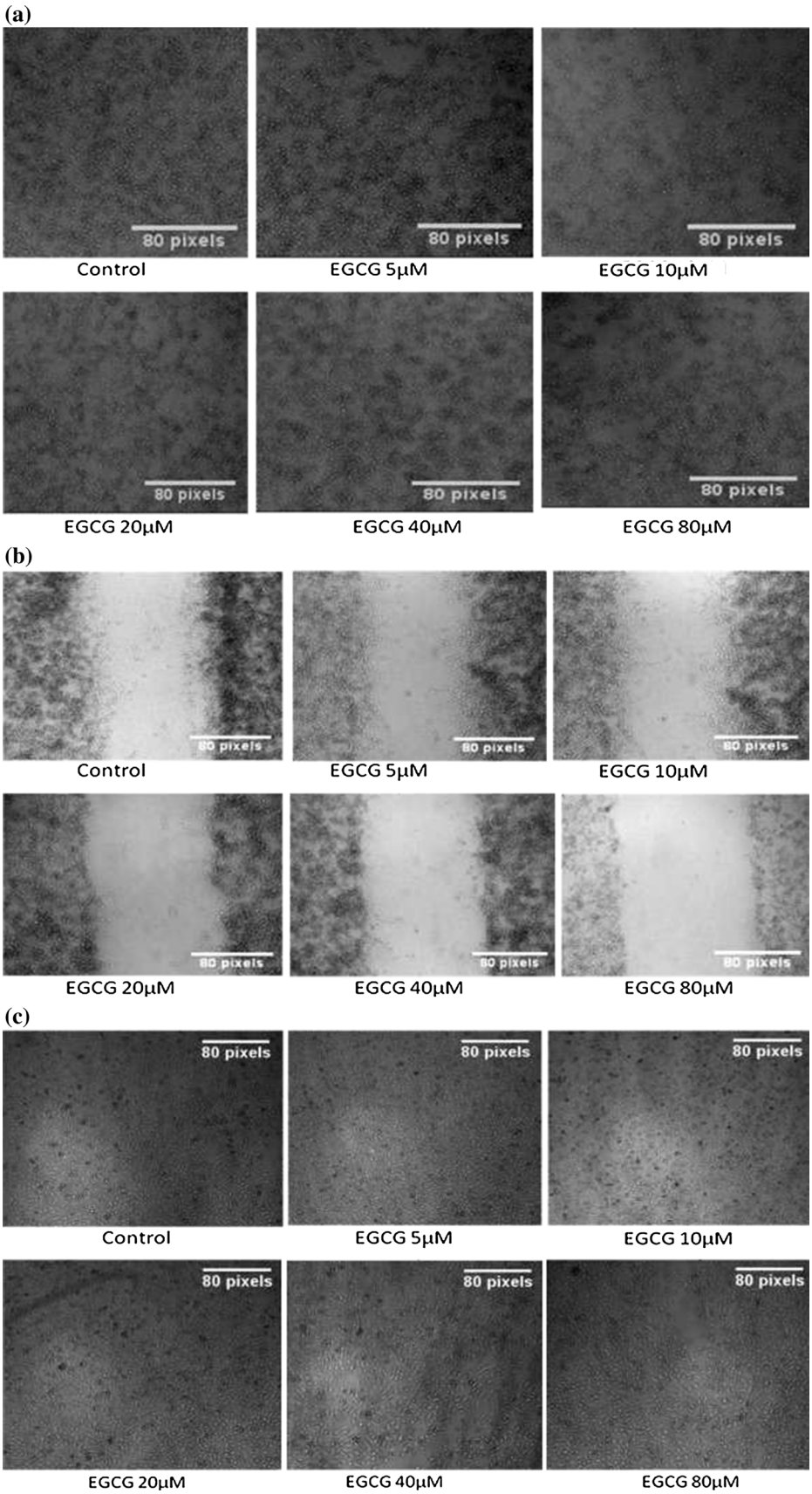

Fig. 7 EGCG reduces cell migration in the HepG2, A549, H460, and PC3 cells determined by wound-healing assay. Representative photomicrographs show morphologic changes of the HepG2 and PC3 cells after the treatment of different concentration of EGCG (**a**, **c**). HepG2 and PC3 cells were seeded in a six-well plate and grown overnight to confluence. After 24 h, cultures were replaced with fresh medium containing 0.5 % FBS (control) or same medium containing concentration-dependant treatment EGCG. Monolayer cells were scratched with a 200-μL pipette tip to create a wound and kept in a 37 °C containing 95 % air and 5 % CO_2. After 48 h, cells were washed twice with DMEM to remove floating cells. The rate of wound closure was photographed after 48 h and adding scale bars to images using ImageJ (**b**, **d**). **e** Figure shows that width of wound increases effectively after the treatment of EGCG for 48 h in all selected *cell lines*. $*P < 0.05$, $**P < 0.01$, and $***P < 0.001$ versus controls

Journal : Large 12032 Dispatch : 19-8-2015 Pages : 18
Article No. : 678 ☐ LE ☐ TYPESET
MS Code : MEDO-D-15-02328 ☑ CP ☑ DISK

Fig. 7 continued

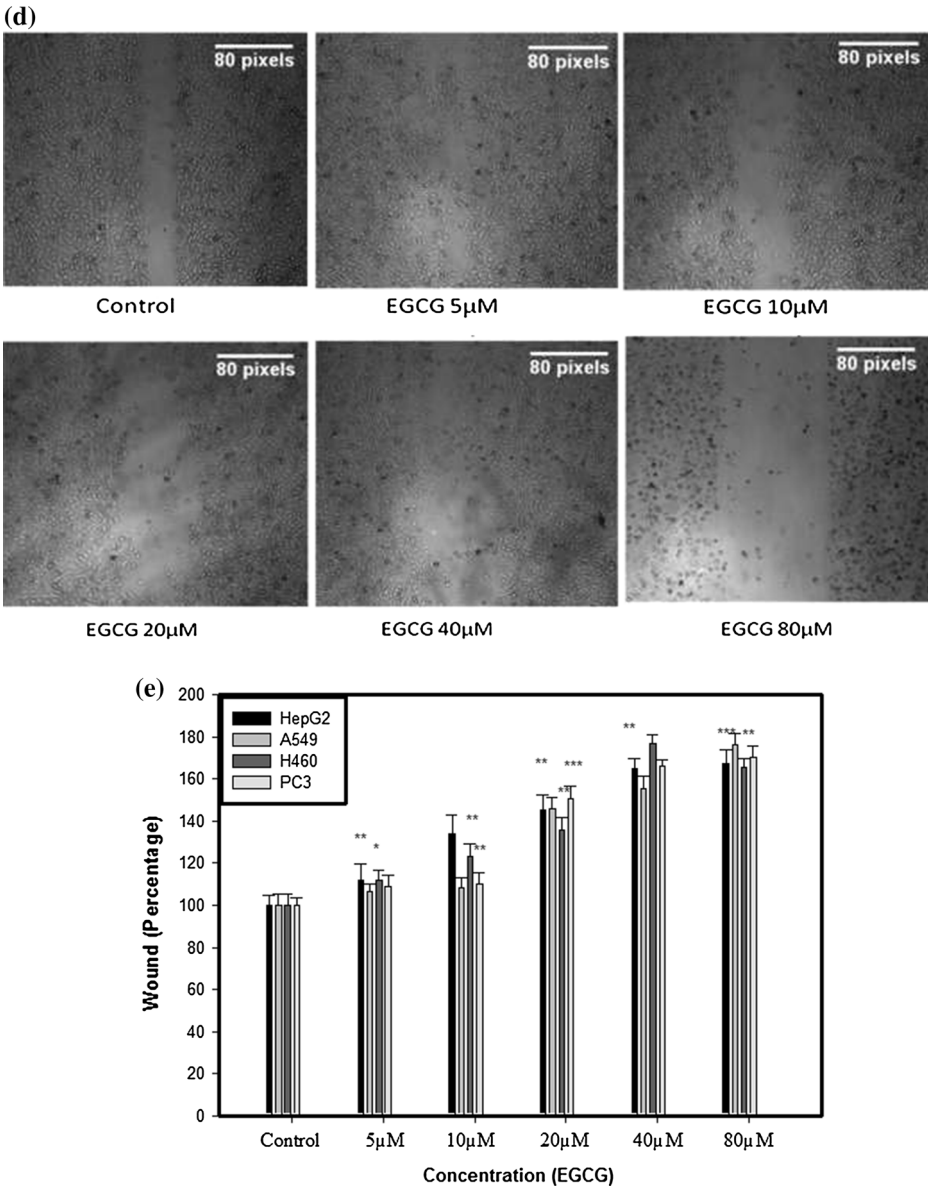

Molecular docking of compounds with androgen receptors (AR) and estrogen receptors (ER)

The androgen receptors (AR) and estrogen receptor (ER) belong to nuclear steroid receptors superfamily, over-expressed in various cancer tissues and elevated tumorigenesis and metastasis in number of cancers including prostate, bladder, lung, breast, and liver [42, 43]. Moreover, AR/ER has a potential to cross-talk with growth factor signaling that regulates cell cycle, apoptosis, and differentiation in cancer cells [44]. A cross-talk between the AR/ER and RTKs in the downstream signaling pathways leads to an increase tissue-specific cell proliferation which is associated with the risk of various cancers [45–50]. Thus, we performed molecular docking study of AR/ER against selected natural compounds. Molecular docking results indicate that the EGCG has better Gscore when docked with AR than previously available AR inhibitor drugs such as bicalutamide and nilutamide. Interestingly, Gscore for EGCG, when docked with the androgen receptor (AR), is −9.95 kcal/mol, and this is better than previously available AR inhibitor, whereas when docked with ER it is −7.73 kcal/mol. Furthermore, protein–ligand interactions of AR (PDB, 2PIV) with EGCG stated that amino acids Leu701, Leu704, Leu707, Trp741, Phe764, Leu873, Met880, Met887, and Phe891 form hydrophobic interactions. Amino acids Leu701, Asp705, and Thr877 were included in side-chain hydrogen bonding, and amino acid Phe764 was involved in backbone hydrogen bonding, whereas amino acid Phe764 was participating in pi–pi

Journal : Large 12032 Dispatch : 19-8-2015 Pages : 18
Article No. : 678 LE TYPESET
MS Code : MEDO-D-15-02328 CP DISK

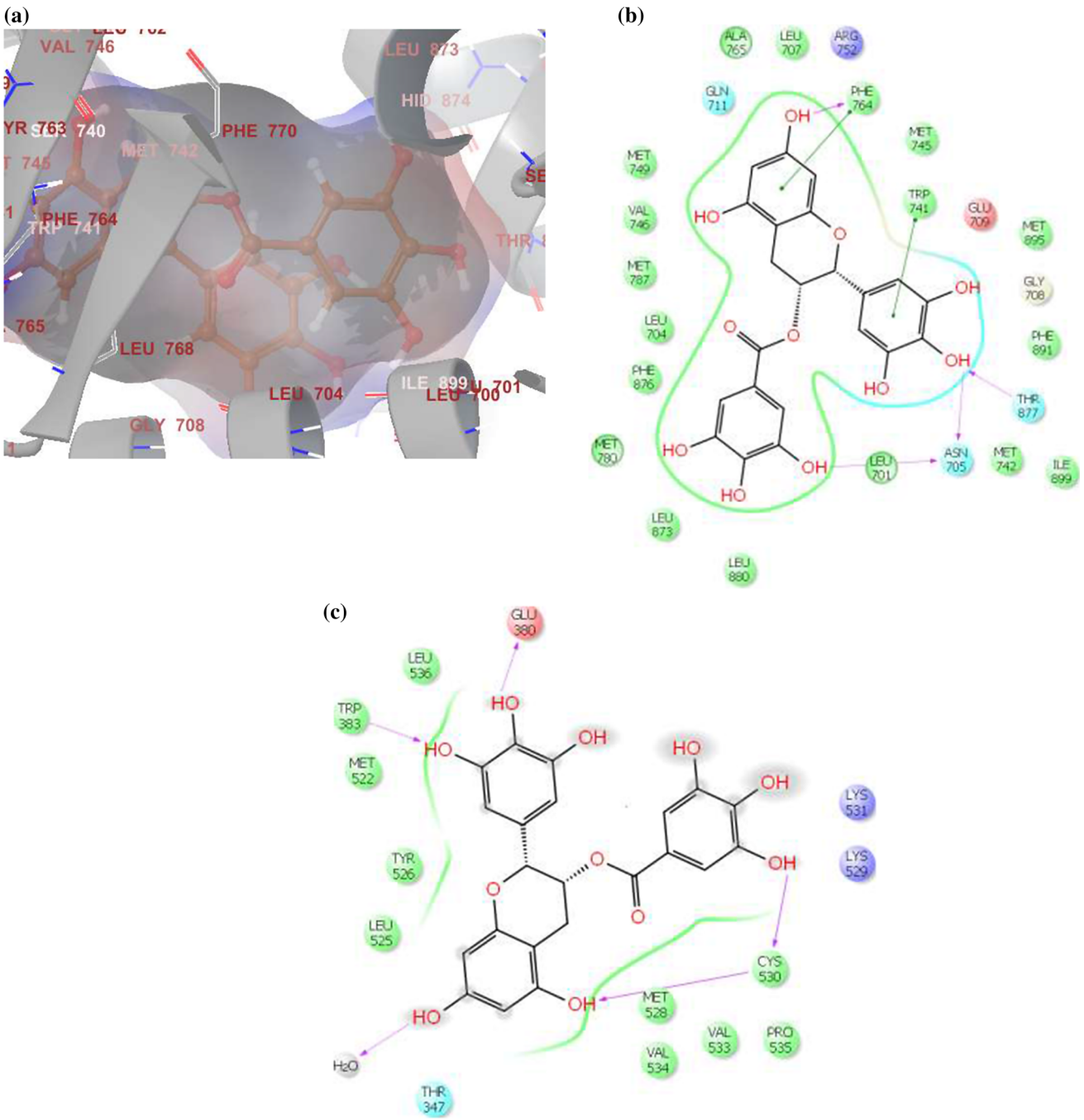

Fig. 8 **a** *Ribbon* presentation of AR (PDB; 2PIV) protein molecule with CID65064, **b** protein–ligand interactions profile of 2PIV with CID65064, **c** protein–ligand interactions profile of ER (PDB, 3ERT) with CID65064

interactions (Table 5 and Fig. 8). Moreover, protein–ligand interactions of ER (PDB, 3ERT) with EGCG revealed that amino acids Met522, Leu525, Tyr526, Met528, Val533, Val534, Pro535, and Leu536 form hydrophobic interactions. Amino acid Trp383 was included in side-chain hydrogen bonding, and amino acid Cys530 was involved in backbone hydrogen bonding (Table 6). It is reported that EGCG adequately inhibits the AR biological effects by the direct antagonist of AR activity [51, 52]. Taken together, our results showed that docking free energy yielded an excellent dock score for EGCG when docked with proteins IGF1R, VEGFR-2, and AR/ER. Moreover, RTKs inhibitors have played an increasingly important role in the treatment of various cancers. Recently published phase clinical III trials have shown terrible efficacies of these drugs. Multi-targeted TKIs have been regarded as promising for various

Journal : Large 12032 Dispatch : 19-8-2015 Pages : 18
Article No. : 678 LE TYPESET
MS Code : MEDO-D-15-02328 CP DISK

Table 5 Lowest binding energy for the ligand–AR (PDB, 2PIV) protein interaction as detected by GLIDE molecular docking

Ligand type	Compounds ID	Gscore	Lipophilic Evdw	H bond	Electro	Protein–ligand interaction
AR inhibitors	CID2375	−5.87	−5.87	−0.85	0	Asn705, Phe764, and Thr 877
	CID4493	−5.37	−4.14	−0.36	−0.21	Asn705, Phe764, and Thr 877
	CID65064	−9.95	−5.4	−4.26	−1.54	Leu701,Asn705, Phe764, and Thr 877

Table 6 Lowest binding energy for the ligand–ER (PDB, 3ERT) protein interactions as detected by Maestro

Ligand type	Compounds ID	Gscore	Lipophilic Evdw	H bond	Electro	Protein–ligand interactions
ER inhibitors	CID449459	−10.4	−7.04	−0.87	−1.02	Glu353 and Arg394
	CID104741	−9.72	−5.82	−0.79	−0.99	Glu353 and Arg394
	CID65064	−7.73	−2.88	−3.56	−1.35	Glu380, Trp383 and Cys530

Molecule CID: pubchem IDs

Gscore: glide extra precision scores (kcal/mol)

Lipophilic E Vdw: chemscore lipophilic pair term and fraction of the total protein–ligand vdw energy

HBond: hydrogen bonding term

Electro: electrostatic rewards

Protein–ligand interaction; π–π stacking, π–cat interaction and hydrogen bond between the ligands and proteins

cancers due to their potential antitumor mechanisms. Single-targeted drugs have poor efficiencies for most cancer patients while they may be highly productive in certain cancer patients. Cancer is an extremely heterogeneous malignancy, with its signal pathways evincing a complex array of cross-signaling pathways. Appropriately, when blocking the targeted pathways, the single-targeted drugs can also be actuated by interconnected signaling pathways that led to increasing cell proliferation. Therefore, the multi-targeted drugs have the better mechanism of action. However, the outcomes endure disappointing if they appertain nonselectively in cancer patients. Further in vitro and in vivo studies are required for the experimental validation of our findings in AR active cells such as prostate cancer cells (LNCaP) and ER^+ breast tumor cell lines.

Conclusion

Docking free energy yielded an excellent dock score for EGCG when docked with proteins IGF1R, VEGFR-2, and AR/ER. Protein–ligand interactions profile underlined that the lipophilic, hydrogen bonding, π–π stacking, and π–cation interactions play a notable contribution in protein–ligand interactions at the active site. Nevertheless, this study tremendously introduces novel classes of multi-target natural compounds. Information obtained from these studies can prove to be useful to fathom the protein–ligand interactions that are required to strengthen the cell growth repressive activity, as well as ameliorated ADME/T properties. Moreover, EGCG reduces the cell proliferation, oxidative stress, and mRNA expression of IGF1R, VEGFRII, mTOR, and Bcl-2. However, further in vitro and in vivo experimental studies are necessitated for the circumstantial mechanism of action of EGCG.

Acknowledgments We would like to thank Vice Chancellor, Central University of Punjab, Bathinda, Punjab, (India) for supporting this study with infrastructural requirements. We also thank Professor P. Ramarao (Dean, Academic Affairs), Central University of Punjab, Bathinda, Punjab, India, for his suggestions during the course that tremendously helped to improve this article. This study was also supported by a Senior Research Fellowship Grant-in-Aid from Indian Council of Medical Research (ICMR), Government of India awarded to PS.

Compliance with ethical standards

Conflict of interest The authors declare that there is no conflict of interests regarding the publication of this article.

References

1. Persidis A. Cancer multidrug resistance. Nat Biotechnol. 1999;17(1):94–5.
2. Costantino L, Barlocco D. Challenges in the design of multitarget drugs against multifactorial pathologies: a new life for medicinal chemistry. Future Med Chem. 2013;5(1):5–7.
3. Landis-Piwowar K, Chen D, Foldes R, Chan T-H, Dou QP. Novel epigallocatechin gallate analogs as potential anticancer agents: a patent review (2009-present). Expert Opin Ther Pat. 2013;23(2):189–202.
4. Khan N, Adhami VM, Mukhtar H. Apoptosis by dietary agents for prevention and treatment of prostate cancer. Endocr Relat Cancer. 2010;17(1):R39–52.

Journal : Large 12032 Dispatch : 19-8-2015 Pages : 18
Article No. : 678 ☐ LE ☐ TYPESET
MS Code : MEDO-D-15-02328 ☑ CP ☑ DISK

5. Nagle DG, Ferreira D, Zhou Y-D. Epigallocatechin-3-gallate (EGCG): chemical and biomedical perspectives. Phytochemistry. 2006;67(17):1849–55.
6. Hsu C-H, Tsai T-H, Kao Y-H, Hwang K-C, Tseng T-Y, Chou P. Effect of green tea extract on obese women: a randomized, double-blind, placebo-controlled clinical trial. Clin Nutr. 2008;27(3):363–70.
7. Singh P, Alex JM, Bast F. Insulin receptor (IR) and insulin-like growth factor receptor 1 (IGF-1R) signaling systems: novel treatment strategies for cancer. Med Oncol. 2014;31(1):1–14.
8. Li J, Zhou N, Luo K, Zhang W, Li X, Wu C, et al. In silico discovery of potential VEGFR-2 inhibitors from natural derivatives for anti-angiogenesis therapy. Int J Mol Sci. 2014;15(9):15994–6011.
9. Yim-Im W, Sawatdichaikul O, Semsri S, Horata N, Mokmak W, Tongsima S, et al. Computational analyses of curcuminoid analogs against kinase domain of HER2. BMC Bioinform. 2014;15(1):1–13.
10. X-q Sun, Chen L, Y-z Li, W-h Li, Liu G-x, Tu Y-q, et al. Structure-based ensemble-QSAR model: a novel approach to the study of the EGFR tyrosine kinase and its inhibitors. Acta Pharmacol Sin. 2014;35(2):301–10.
11. Liu L, Leung K, Chan DS, Wang Y, Ma D, Leung C. Identification of a natural product-like STAT3 dimerization inhibitor by structure-based virtual screening. Cell Death Dis. 2014;5(6):e1293.
12. Mayer AM, Gustafson KR. Marine pharmacology in 2005–2006: antitumour and cytotoxic compounds. Eur J Cancer. 2008;44(16):2357–87.
13. Mayer AM, Gustafson KR. Marine pharmacology in 2001–2: antitumour and cytotoxic compounds. Eur J Cancer. 2004;40(18):2676–704.
14. Robinson DR, Wu Y-M, Lin S-F. The protein tyrosine kinase family of the human genome. Oncogene. 2000;19(49):5548–57.
15. da Rocha AB, Lopes RM, Schwartsmann G. Natural products in anticancer therapy. Curr Opin Pharmacol. 2001;1(4):364–9.
16. Sunil H. Inhibition studies of naturally occurring terpene based compounds with cyclin-dependent kinase 2 enzyme. J Comput Sci Syst Biol. 2012;5:2.
17. Sarkar FH, Li Y. Using chemopreventive agents to enhance the efficacy of cancer therapy. Cancer Res. 2006;66(7):3347–50.
18. Hillman GG. Dietary agents in cancer chemoprevention and treatment. J Oncol. 2012. doi:10.1155/2012/749310.
19. Phosrithong N, Ungwitayatorn J. Molecular docking study on anticancer activity of plant-derived natural products. Med Chem Res. 2010;19(8):817–35.
20. Cho JY, Park J. Contribution of natural inhibitors to the understanding of the PI3 K/PDK1/PKB pathway in the insulin-mediated intracellular signaling cascade. Int J Mol Sci. 2008;9(11):2217–30.
21. Singh P, Bast F. Multitargeted molecular docking study of plant-derived natural products on phosphoinositide-3 kinase pathway components. Med Chem Res. 2014;23(4):1690–700.
22. Singh P, Bast F. Screening and biological evaluation of myricetin as a multiple target inhibitor insulin, epidermal growth factor, and androgen receptor; in silico and in vitro. Invest New Drugs. 2015;33(3):575–93.
23. Singh P, Bast F. In silico molecular docking study of natural compounds on wild and mutated epidermal growth factor receptor. Med Chem Res. 2014;23(12):5074–85.
24. Singh P, Bast F. High-throughput virtual screening, identification and in vitro biological evaluation of novel inhibitors of signal transducer and activator of transcription 3. Med Chem Res. 2015;24(6):2694–708.
25. Friesner RA, Murphy RB, Repasky MP, Frye LL, Greenwood JR, Halgren TA, et al. Extra precision glide: docking and scoring incorporating a model of hydrophobic enclosure for protein-ligand complexes. J Med Chem. 2006;49(21):6177–96.
26. Halgren TA, Murphy RB, Friesner RA, Beard HS, Frye LL, Pollard WT, et al. Glide: a new approach for rapid, accurate docking and scoring 2. Enrichment factors in database screening. J Med Chem. 2004;47(7):1750–9.
27. Friesner RA, Banks JL, Murphy RB, Halgren TA, Klicic JJ, Mainz DT, et al. Glide: a new approach for rapid, accurate docking and scoring 1. Method and assessment of docking accuracy. J Med Chem. 2004;47(7):1739–49.
28. Lu JJ, Crimin K, Goodwin JT, Crivori P, Orrenius C, Xing L, et al. Influence of molecular flexibility and polar surface area metrics on oral bioavailability in the rat. J Med Chem. 2004;47(24):6104–7.
29. Jorgensen WL, Duffy EM. Prediction of drug solubility from structure. Adv Drug Deliv Rev. 2002;54(3):355–66.
30. Mechoulam H, Pierce EA. Expression and activation of STAT3 in ischemia-induced retinopathy. Invest Ophthalmol Vis Sci. 2005;46(12):4409–16.
31. Hwang YP, Jeong HG. Metformin blocks migration and invasion of tumour cells by inhibition of matrix metalloproteinase-9 activation through a calcium and protein kinase Cα-dependent pathway: phorbol-12-myristate-13-acetate-induced/extracellular signal-regulated kinase/activator protein-1. Br J Pharmacol. 2010;160(5):1195–211.
32. Lee S-H, Zahoor M, Hwang J-K, Choi K-Y. Valproic acid induces cutaneous wound healing in vivo and enhances keratinocyte motility. PLoS ONE. 2012;7(11):e48791.
33. Gu J-W, Makey KL, Tucker KB, Chinchar E, Mao X, Pei I, et al. EGCG, a major green tea catechin suppresses breast tumor angiogenesis and growth via inhibiting the activation of HIF-1α and NFκB, and VEGF expression. Vasc Cell. 2013;5(1):9.
34. Zhou J, Farah BL, Sinha RA, Wu Y, Singh BK, Bay B-H, et al. Epigallocatechin-3-gallate (EGCG), a green tea polyphenol, stimulates hepatic autophagy and lipid clearance. PLoS ONE. 2014;9(1):e87161.
35. Manohar M, Fatima I, Saxena R, Chandra V, Sankhwar PL, Dwivedi A. (−)-Epigallocatechin-3-gallate induces apoptosis in human endometrial adenocarcinoma cells via ROS generation and p38 MAP kinase activation. J Nutr Biochem. 2013;24(6):940–7.
36. Punathil T, Tollefsbol TO, Katiyar SK. EGCG inhibits mammary cancer cell migration through inhibition of nitric oxide synthase and guanylate cyclase. Biochem Biophys Res Commun. 2008;375(1):162–7.
37. Chang C-W, Hsieh Y-H, Yang W-E, Yang S-F, Chen Y, Hu D-N. Epigallocatechingallate inhibits migration of human uveal melanoma cells via downregulation of matrix metalloproteinase-2 activity and ERK1/2 pathway. BioMed Res Int. 2014. doi:10.1155/2014/141582.
38. Chen Y-J, Cheng Y-J, Hung AC, Wu Y-C, Hou M-F, Tyan Y-C, et al. The synthetic flavonoid WYC02-9 inhibits cervical cancer cell migration/invasion and angiogenesis via MAPK14 signaling. Gynecol Oncol. 2013;131(3):734–43.
39. Shimizu M, Adachi S, Masuda M, Kozawa O, Moriwaki H. Cancer chemoprevention with green tea catechins by targeting receptor tyrosine kinases. Mol Nutr Food Res. 2011;55(6):832–43.
40. Shimizu M, Shirakami Y, Moriwaki H. Targeting receptor tyrosine kinases for chemoprevention by green tea catechin EGCG. Int J Mol Sci. 2008;9(6):1034–49.
41. Yuan J, Liu H, Kang X, Zou G. Molecular docking of epidermal growth factor receptor tyramine kinase domain and its inhibitor genistein. Chin J Biotechnol. 2008;24(10):1813–7.
42. Chang C, Lee S, Yeh S, Chang T. Androgen receptor (AR) differential roles in hormone-related tumors including prostate,

Journal : Large 12032 Dispatch : 19-8-2015 Pages : 18
Article No. : 678 ☐ LE ☐ TYPESET
MS Code : MEDO-D-15-02328 ☑ CP ☑ DISK

bladder, kidney, lung, breast and liver. Oncogene. 2013;33 (25):3225–34.
43. Lonergan PE, Tindall DJ. Androgen receptor signaling in prostate cancer development and progression. J Carcinogen. 2011;10(1):20.
44. Zhu M-L, Kyprianou N. Androgen receptor and growth factor signaling cross-talk in prostate cancer cells. Endocr Relat Cancer. 2008;15(4):841–9.
45. Wang Y, Kreisberg JI, Ghosh PM. Cross-talk between the androgen receptor and the phosphatidylinositol 3-kinase/Akt pathway in prostate cancer. Curr Cancer Drug Targets. 2007;7(6):591–604.
46. Naderi A, Hughes-Davies L. A functionally significant cross-talk between androgen receptor and ErbB2 pathways in estrogen receptor negative breast cancer. Neoplasia. 2008;10(6):542.
47. Craft N, Shostak Y, Carey M, Sawyers CL. A mechanism for hormone-independent prostate cancer through modulation of androgen receptor signaling by the HER-2/neu tyrosine kinase. Nat Med. 1999;5(3):280–5.
48. Lee AV, Cui X, Oesterreich S. Cross-talk among estrogen receptor, epidermal growth factor, and insulin-like growth factor signaling in breast cancer. Clin Cancer Res. 2001;7(12):4429s–35s.
49. Levin ER. Bidirectional signaling between the estrogen receptor and the epidermal growth factor receptor. Mol Endocrinol. 2003;17(3):309–17.
50. Liu C, Zhang Z, Tang H, Jiang Z, You L, Liao Y. Crosstalk between IGF-1R and other tumor promoting pathways. Curr Pharm Des. 2014;20(17):2912–21.
51. Siddiqui IA, Asim M, Hafeez BB, Adhami VM, Tarapore RS, Mukhtar H. Green tea polyphenol EGCG blunts androgen receptor function in prostate cancer. FASEB J. 2011;25(4):1198–207.
52. Farabegoli F, Barbi C, Lambertini E, Piva R. (−)-Epigallocatechin-3-gallate downregulates estrogen receptor alpha function in MCF-7 breast carcinoma cells. Cancer Detect Prev. 2007;31(6):499–504.

Journal : Large 12032 Dispatch : 19-8-2015 Pages : 18
Article No. : 678 ☐ LE ☐ TYPESET
MS Code : MEDO-D-15-02328 ☑ CP ☑ DISK